Novel Magnetic Carbon Nanotube-TiO$_2$ Composites for Solar Light Photocatalytic Degradation of Pharmaceuticals in the Presence of Natural Organic Matter

Dion Awfa[a], Mohamed Ateia[b,*], Manabu Fujii[a], Chihiro Yoshimura[a]

[a] Department of Civil and Environmental Engineering, School of Environment and Society, Tokyo Institute of Technology, 2-12-1, M1-4, Ookayama, Meguro-ku, Tokyo 152-8552, Japan
[b] Department of Environmental Engineering and Earth Sciences, Clemson University, Clemson, SC 29634, United States

ABSTRACT

Magnetic carbon nanotube-TiO$_2$ (MCNT-TiO$_2$) composites that rely on the inherent magnetic properties of carbon nanotubes were synthesized and their photocatalytic activity was evaluated for the degradation of carbamazepine and sulfamethoxazole under solar irradiation and environmentally relevant conditions. Compared with a TiO$_2$ reference catalyst, the MCNT-TiO$_2$ composites exhibited a higher photodegradation rate due to the high surface area and extended visible light absorption. The photodegradation rate constants for carbamazepine and sulfamethoxazole in pure water were ~1.5 and ~1.2 times greater than those for TiO$_2$, respectively. The catalysts were tested in the presence of natural organic matter and rapid photodegradation rates for carbamazepine and sulfamethoxazole were observed relative to bare TiO$_2$, indicating that MCNT-TiO$_2$ may be suitable for practical applications. Solar and UVC reactivation were used to recover the photocatalytic activity, and UVC irradiation was more efficient and maintained the performance of MCNT-TiO$_2$ for consecutive treatment cycles. MCNT-TiO$_2$ with its unique fast kinetics and high photodegradation activity toward micropollutants exhibits great potential as an alternative method for water and wastewater treatment.

1. Introduction

Effluents from municipal and industrial wastewater treatment plants are the main source of pharmaceuticals in natural waters [1,2]. Pharmaceutical concentrations as low as $500 \, \text{ng L}^{-1}$ in natural water could alter the reproduction and tissue regeneration of living organisms [3–5]. The production and consumption of pharmaceuticals have increased dramatically over the past few decades. However, current wastewater treatment technologies (e.g., activated sludge) are not effective in removing these harmful compounds [6]. The antiepileptic carbamazepine and the antibiotic sulfamethoxazole are the most frequently detected persistent pharmaceuticals worldwide in natural and waste water [7], and their average removal efficiencies in water treatment plants are below 20% and 55%, respectively [6]. Therefore, efficient water treatment techniques are needed to reduce the release of pharmaceuticals into the aquatic environment.

Photocatalysis is a promising advanced water treatment process for degrading pharmaceuticals that may be suitable to replace or assist conventional treatment approaches [8–10]. TiO$_2$ is the most widely used semiconductor for photocatalytic processes due to its low cost, non-toxicity, and high stability [11]. In addition, carbon nanotube (CNT)-TiO$_2$ composites have attracted attention for environmental applications for several reasons. CNTs concentrate the contaminants by adsorption, bringing the contaminants closer to the TiO$_2$ active sites for photodegradation [12]. Combining CNTs with TiO$_2$ can promote the separation of the electron-hole charges generated upon irradiation, and the presence of C-O-Ti linkages reduces the band gap, and thus extends the absorption wavelength [13]. Previous studies of CNT-TiO$_2$ have not used practical water treatment conditions, such as the presence of background natural organic matter (NOM) (Table S1). Most experimental studies of CNT-TiO$_2$ photocatalysis have focused on the kinetics and mechanisms for individual contaminants at high pharmaceutical concentrations ($10–100 \, \text{mg L}^{-1}$) that are 10^4–10^5 times higher than their practical concentrations [14]. The coexistence of NOM reduces the photocatalytic activity of TiO$_2$ because NOM is present in natural waters and wastewater at concentrations several orders of magnitude higher than pharmaceuticals. Thus, NOM interferes with the photocatalytic mechanisms via the inner filter effect and radical scavenging,

and adsorbed NOM competes for active sites with the targeted pollutants [15–17]. The photocatalytic activity increases with the increase in the number of active reaction sites and the lifetime of photogenerated electron/hole pairs, which results in higher radical generation [14]. Hence, increasing the specific surface area for photocatalytic reaction sites in CNT-TiO$_2$ would reduce the probability of electron/hole pair recombination and minimize the inhibitory effect of NOM.

In this study, we used the inherently magnetic particles present in pristine CNTs as a green, facile approach to prepare magnetic carbon nanotubes (MCNTs) [18]. Our facile method is also scalable, inexpensive, and preserves the external surface of the nanotube walls for TiO$_2$ particles. We investigated the photocatalytic activity of a MCNT-TiO$_2$ composite in the presence of NOM, which is more relevant to conditions in water treatment plants. We used industrial grade CNTs to prepare MCNT-TiO$_2$ by a simple mixing method. Industrial grade CNTs was chosen due to its significant lower cost and higher content of metallic residuals (i.e., magnetic particles) compared to the analytical grade CNTs. The photocatalytic activity of MCNT-TiO$_2$ for the photodegradation of carbamazepine and sulfamethoxazole was tested under solar light irradiation with and without NOM, and we compared solar and UVC irradiation photooxidation reactivation techniques for regenerating MCNT-TiO$_2$. Further, electrical energy demand (E$_{EO}$) was calculated for the evaluation of energy-efficiencies of the new material at relevant environmental conditions.

2. Materials and methods

2.1. Materials

Carbamazepine ($\geq$98%, molecular formula C$_{15}$H$_{12}$N$_2$O, molecular weight 236.269 g mol^{-1}), sulfamethoxazole ($\geq$98%, molecular formula C$_{10}$H$_{11}$N$_3$O$_3$S, molecular weight 253.279 g mol^{-1}), Aeroxide P25 TiO$_2$ ($\geq$99.5%, Brunauer-Emmet-Teller [BET] specific surface area 35–65 m^2 g^{-1}, average particle size < 21 nm), high-performance liquid chromatography (HPLC) grade methanol ($\geq$99.8%), and acetonitrile ($\geq$99.8%) were purchased from Sigma-Aldrich (Japan). Industrial grade multi-walled CNTs (> 90%, diameter 10–20 nm, length 10–30 μm, BET specific surface area 201 m^2 g^{-1}) were obtained from Chengdu Alpha Nano Technology (China). A permanent Nd-Fe-B magnet was purchased from Magna Co. (Japan). Ethanol, HCl, and NaOH were sourced from Kanto Chemical (Japan). Upper Mississippi River NOM (URNOM) was obtained from International Humic Substances Society (USA), and the chemical properties of URNOM are shown in Table S2. All reagents were of analytical grade and were used as received. Stock solutions of 10 mg L^{-1} carbamazepine and sulfamethoxazole were prepared in ultrapure water (18.2 MΩ cm^{-1}). The URNOM sample was dissolved in 0.01 M NaOH solution to prepare a 10 g L^{-1} NOM stock solution, and then the pH was adjusted to 7.0 $\pm$ 0.2 using 0.01 M HCl solution. The volume of acid or alkali solution was recorded and was considered when calculating the final NOM concentration. All stock solutions were stored at 4 °C in the dark when not in use.

2.2. Preparation and characterization of MCNT-TiO$_2$ composites

MCNTs were prepared using a facile method described in our previous work [18,19]. As-received CNTs (0.5 g) were dispersed in ethanol (100 mL) with a sonicator. The magnetic fraction of CNTs was separated with the permanent Nd-Fe-B magnet, and the non-magnetic and low-magnetism fractions were decanted. This procedure was repeated three times with ethanol followed by three times with water. The MCNTs were dried in an oven at 105 °C for 24 h, and stored at room temperature prior to use. The MCNT-TiO$_2$ composite was prepared by a simple mixing method with some modifications [20–23]. The MCNTs were dispersed in ethanol and sonicated for 60 s (**solution A**). TiO$_2$ nanoparticles were dispersed in ethanol and sonicated for 60 s

(**solution B**). A mixture of **solutions A** and **B** was sonicated for 60 s followed by mixing with a magnetic stirrer for 12 h. The MCNT-TiO$_2$ composite was separated from the solution with a permanent magnet (Fig. S1), washed with ethanol and with water, dried at 105 °C overnight, and stored prior to use. MCNT-TiO$_2$ composites were prepared with MCNT:TiO$_2$ mass ratios of 10:1, 5:1, 1:1, 1:5, and 1:10. The carbon contents in the MCNTs and the MCNT-TiO$_2$ composites were determined using a gravimetry method by calcining the samples at 700 °C for 2 h [24].

The crystallinities of the composites were determined by X-ray diffraction (XRD) with an X-ray powder diffractometer (MiniFlex 600, Rigaku, Japan) using Cu Kα (λ = 1.5406 Å) radiation and over a 2θ range of 10–80°. Samples morphologies were analyzed by field emission scanning electron microscopy (SEM; SU9000, Hitachi, Japan). Transmission electron microscopy-energy dispersive X-ray spectroscopy (TEM-EDX) was used to observe the microstructure and elemental composition of the samples (JEM-2010 F, JEOL, Japan). The specific surface area was measured by the BET method and the pore volumes were determined from nitrogen adsorption data at 77 K obtained with a surface area analyzer (ASAP 2020, Micromeritics, Japan). The magnetic activity of the samples was measured by using a vibrating sample magnetometer (BHV-50 V, Riken Denshi, Japan). All of the magnetization results were normalized to the total weight of the sample. FTIR spectra (FTIR 4600, JASCO, Japan) were measured in the range of 400 to 4000 cm^{-1} using a KBr plate.

2.3. Adsorption and photocatalytic degradation experiments

The photocatalytic degradation of carbamazepine and sulfamethoxazole (150–500 μg L^{-1}) were studied in a glass beaker in aqueous solution (200 mL). The concentrations were chosen based on reported concentrations of carbamazepine and sulfamethoxazole in water and wastewater [25]. The pH values of the solutions were adjusted to 7.0 $\pm$ 0.2 with 0.01 M HCl and NaOH. The concentration of the catalyst (TiO$_2$, MCNTs, and MCNT-TiO$_2$ composites) was 0.1 g L^{-1}. The temperature was kept constant at room temperature (26 $\pm$ 3 °C). A solar simulator (MS-35AAA, Ushio Lighting Edge Technologies, Japan) at an intensity of 1000 W m^{-2} was used as a light source [26]. Each photocatalysis experiment consisted of two steps. i) Adsorption of carbamazepine and sulfamethoxazole on the catalyst surface for 60 min in the dark with or without NOM to reach adsorption-desorption equilibrium. Additional stirring for 120 min resulted in no further adsorption. ii) Photocatalytic degradation of carbamazepine and sulfamethoxazole with or without NOM under irradiation from the solar simulator.

The photocatalytic activity of the composites was investigated in the presence of NOM by spiking the solution with URNOM and the dissolved organic carbon (DOC) was adjusted to 5 mg L^{-1}, which is the average concentration in surface water and pre-treated domestic wastewater [27,28]. Under dark conditions, samples were collected at 5, 10, 15, 30, 50, and 60 min. During irradiation, the reaction solutions were stirred continuously and aliquots of the samples were collected at 5, 10, 15, 20, and 30 min. Blank experiments without catalysts were run to test the photolysis of carbamazepine and sulfamethoxazole in ultrapure water and in the presence of NOM for 30 min. All of the experiments were run in duplicate.

2.4. Recyclability of MCNT-TiO$_2$ composites

The recyclability of MCNT-TiO$_2$ was tested without NOM. Two different recyclability scenarios were tested. In the first, the spent MCNT-TiO$_2$ after the photocatalytic degradation reaction was collected with a permanent magnet to separate it from the solution. The MCNT-TiO$_2$ was then used directly for the next photocatalysis cycles. In the second scenario, xenon short-arc lamp and UVC (λ = 254 nm, 80 W m^{-2}) lamp irradiation were used for photooxidation reactivation. The spent MCNT-TiO$_2$ was collected with a permanent magnet, placed in

ultrapure water, and exposed to solar or UVC irradiation for 1 h. The photooxidation-reactivated MCNT-TiO$_2$ composites were used for the next cycle of photocatalysis under solar irradiation, as described in Section 2.3. The weight loss of MCNT-TiO$_2$ after the recyclability experiments was negligible.

2.5. Analytical and statistical methods

The carbamazepine and sulfamethoxazole concentrations were analyzed using an HPLC system (Prominence UFLC, Shimadzu, Japan) equipped with a UV–vis absorbance detector (SPD-20 UFLC, Shimadzu) and a C18 column (Kinetex, Phenomenex Co., USA; 5 μm, 4.6 × 250 mm). Prior to HPLC analysis, the samples were filtered through a 0.45 μm membrane filter (PES Filter, Membrane Solutions, Japan). DOC concentrations were quantified using total organic carbon (TOC) analyzer (TOC-CHP, Shimadzu V-series, Japan). The analytical methods and their minimum reporting limits are shown in Table S3.

Linear regression analysis was used to examine the relationship between adsorption capacity and specific surface area ($p < 0.05$). One-way analysis of variance (Tukey's mean comparison test, $p < 0.05$) was used to compare photocatalytic activity (k_{app}) for different catalysts and different recyclability scenarios. Student's t-test at a 5% significance level was used to compare the effect of initial concentrations and the presence of NOM for both TiO$_2$ and MCNT-TiO$_2$.

2.6. Calculation of electrical energy per order of the transformation

The energy efficiency of photocatalysis is expressed in terms of electrical energy per order (E_{EO}) of the transformation, and is defined as the electrical energy in kilowatt hours required to degrade a contaminant by one order of magnitude in 1 m^3 of contaminated water [29]. E_{EO} is determined by

$$E_{EO} = \frac{\text{Electrical power(kW)} \times \text{Time(h)}}{\text{Volume(m}^3) \times \log(\frac{C_0}{C_t})} \quad (1)$$

where C_0 and C_t are the initial and final concentrations of each substance (mg L^{-1}).

3. Results and discussion

3.1. Materials characterization

Fig. 1 shows the SEM images of MCNTs, TiO$_2$, and MCNT-TiO$_2$ composites. The number of TiO$_2$ clusters increased in the composites as the MCNT:TiO$_2$ mass ratio decreased. TEM-EDX analysis indicated that there were metallic Co particles inside the tubes and they were the main source of the magnetic activity of MCNTs (Figs. S2 and S3). This is consistent with previous studies on commercial CNTs containing metal impurities (i.e., Fe, Ni, and Co) in the tubes from the production processes, which could give the material inherent magnetic properties [30]. The gravimetric analysis of MCNTs indicated that the magnetic particles accounted for ˜6% of the total MCNT mass (Table 1). Previous MCNT preparation methods that attach magnetic particles (e.g., metal oxides) and TiO$_2$ to the surface of CNT have suffered from photo-dissolution and release of the metals into solution [22,31,32]. However, in our MCNTs, these metallic particles are stable and difficult to remove, even in concentrated acids at high temperature [18]. Moreover, the utilization of industrial grade CNT in this study can decrease the cost for material preparation due to relatively lower price compare to the analytical grade CNT. Therefore, our approach has the extra advantage over previously reported methods of avoiding unintentional contamination of the solution with magnetic particles and low material cost.

The surface area, total pore volume, pore distribution, and magnetization values of MCNTs, TiO$_2$, and MCNT-TiO$_2$ composites are listed in Table 1. The surface area and total pore volume of MCNT-TiO$_2$ composites were higher than those of pristine TiO$_2$, confirming that TiO$_2$ was anchored to the MCNTs, a high-surface-area adsorbent. The specific surface area decreased and the total pore volume of the composite decreased as the TiO$_2$ loading increased. The pore volume distribution for all samples showed that mesopores (50 nm > pore size > 2 nm) and macropores (pore size > 50 nm) were dominant with a small percentage of micropores (< 1%). The pores were formed by TiO$_2$ and MCNT bundles, as both materials are non-porous [33,34]. The magnetization curves showed that all the composites had paramagnetic properties (Fig. S4) [18], and the saturation magnetization values were highest for the MCNTs and decreased with increasing TiO$_2$ fraction in the MCNT-TiO$_2$ composites. However, all composites showed high magnetic activity and responded fast (< 1 min) to an external magnetic field.

XRD diffraction peaks for MCNTs, TiO$_2$, and MCNT-TiO$_2$ composites are shown in Fig. S5. The MCNTs had two main diffraction peaks at $2\theta \approx 26°$ and $43°$ that were attributed to the carbon nanotube graphite-like structure [18]. However, Co particles were not detected in all samples because their concentrations were below the detection sensitivity limit of the XRD measurements [30] and the main diffraction peak of Co ($2\theta \approx 45°$) overlapped with the graphite-like peak ($2\theta \approx 43°$) [35]. The diffraction peak of TiO$_2$ consisted of anatase (main diffraction peak at $2\theta \approx 25.3°$) and rutile (main diffraction peak at $2\theta \approx 27.4°$) TiO$_2$ peaks. Polymorphous TiO$_2$, consisting of a mixture of anatase and rutile TiO$_2$, has better photocatalytic activity and a smaller band gap than the individual phases [36]. For all MCNT-TiO$_2$ composites, the profile and intensity of TiO$_2$ peaks were consistent with the mass ratio of TiO$_2$ in each composite, and an overlap with the MCNT peaks was observed at lower TiO$_2$ masses. The FTIR spectra of the samples are shown in Fig. S6. The broad peaks at 3730 and 3380 cm^{-1} were assigned to O−H stretching. The peaks at 1520 and 970 cm^{-1} arose from C=C stretching and bending vibrations, respectively. In addition, the absorption peak at 690 cm^{-1} was characteristic of C−H. The peak for the Ti−O stretching vibration appeared around 450 cm^{-1} for the TiO$_2$ and MCNT-TiO$_2$ composites [37].

3.2. Adsorption and photodegradation of pharmaceuticals

3.2.1. Adsorption phase

The adsorption of the contaminants on or close to the catalyst surface plays an important role in the effective photodegradation of the contaminants. The increase in the adsorption capacity and pore volume of MCNT-TiO$_2$ can increase the overall photocatalytic activity due to the synergetic effect of adsorption and photocatalysis. At initial carbamazepine and sulfamethoxazole concentrations of 150 μg L^{-1}, all MCNT-TiO$_2$ composites exhibited adsorption equilibria in the range of 1–1.4 mg g^{-1}, which were much higher than that of bare TiO$_2$ (0.2 mg g^{-1}) (Fig. S7). The adsorption equilibrium of the materials was positively correlated with their surface area, as indicated by the R^2 values (> 0.99, $p < 0.001$). The main mechanisms for the adsorption on the surface of TiO$_2$ are the electrostatic attraction and ligand exchange [38]. On the other hand, the presence of the CNT, in case of MCNT-TiO$_2$, enhances the adsorption mechanism via hydrophobic interaction, π-π interaction, hydrogen-bonding interactions, and electrostatic interactions [39]. Carbamazepine is a neutral species; therefore, the mass transport of carbamazepine is mainly governed by hydrophobic and π-π interactions [40]. In contrast, sulfamethoxazole has two acidic dissociation constants of pK$_{a,1} = 1.85$ and pK$_{a,2} = 5.6$ [41], indicating that sulfamethoxazole molecules were present in anionic form under the neutral pH conditions in this study, and the adsorption mechanism onto MCNT-TiO$_2$ and TiO$_2$ could be affected by electrostatic interactions.

3.2.2. Photodegradation phase

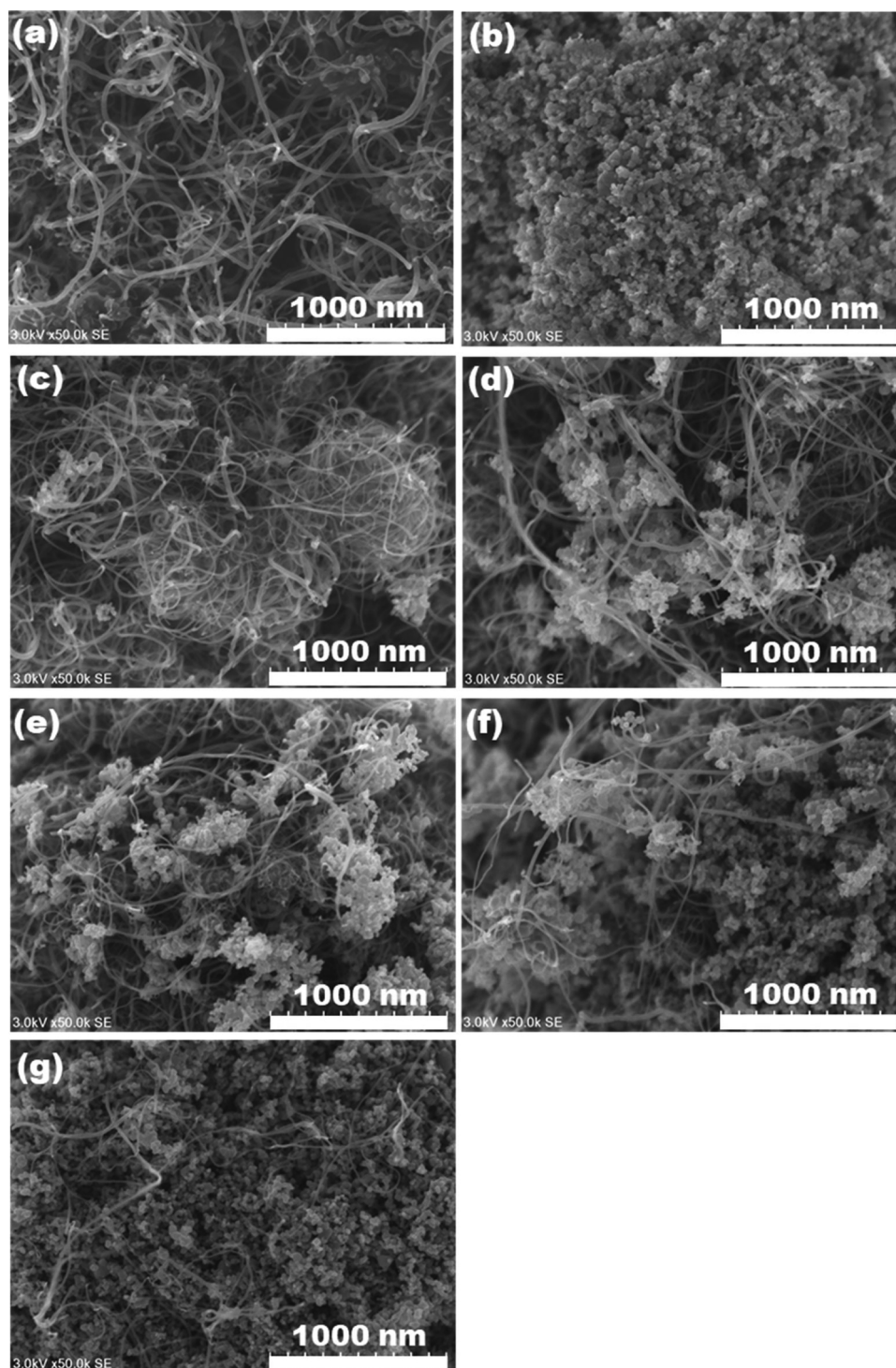The results showed that for direct photolysis without catalysts under

Fig. 1. SEM images of (a) MCNTs, (b) TiO_2, (c) MCNT-$TiO_{2\ (10:1)}$, (d) MCNT-$TiO_{2\ (5:1)}$, (e) MCNT-$TiO_{2\ (1:1)}$, (f) MCNT-$TiO_{2\ (1:5)}$, and (g) MCNT-$TiO_{2\ (1:10)}$. The values in the brackets following the composite name show the MCNT:TiO_2 mass ratio.

solar irradiation, carbamazepine showed negligible removal ($< 2\%$), whereas the sulfamethoxazole concentration decreased significantly by 20–50% (Fig. S8). The carbamazepine removal was negligible under direct photodegradation because it does not have functional groups that absorb radiation at $> 290\ nm$, which is the main solar irradiation spectrum [42]. The higher removal of sulfamethoxazole is related to its phenylamine functional group, which absorbs radiation at $> 290\ nm$ [43]. The photocatalytic degradation for both compounds using all composites was tested. The photodegradation reactions were described quantitively by the Langmuir-Hinshelwood model and the pseudo-first-

order rates (k_{app}) were used to examine the photodegradation efficiencies [44]. k_{app} of carbamazepine followed the trend MCNT-$TiO_{2\ (1:5)}$ > MCNT-$TiO_{2\ (1:10)}$ > TiO_2 $\approx$ MCNT-$TiO_{2\ (1:1)}$ (not significantly different) > MCNT-$TiO_{2\ (5:1)}$ > MCNT-$TiO_{2\ (10:1)}$ ($p < 0.001$) (Fig. 2). The highest carbamazepine photodegradation was observed with MCNT-$TiO_{2\ (1:5)}$ ($k_{app} = 6.8 \times 10^{-2}\ min^{-1}$), which was almost 1.5 times the value for bare TiO_2 ($k_{app} = 4.6 \times 10^{-2}\ min^{-1}$), and the maximum synergetic effect between TiO_2 and MCNT was achieved with MCNT-$TiO_{2\ (1:5)}$. The solar light reactivity of TiO_2 was enhanced significantly in the presence of MCNT due to: 1) the excited MCNT can inject

Table 1
Characteristics of TiO₂, MCNTs, and MCNT-TiO₂ composites used in this study.

Catalysts	Carbon Contents (%)	SA ($m^2 g^{-1}$)	PV_{total} ($cm^3 g^{-1}$) [%]	PV_{micro} ($cm^3 g^{-1}$) [%]	PV_{meso} ($cm^3 g^{-1}$) [%]	PV_{macro} ($cm^3 g^{-1}$) [%]	Magnetization (emu g^{-1})
TiO₂	–	56	0.24 [100]	0.002 [0.8]	0.13 [53.7]	0.11 [45.5]	–
MCNT	94	201	1.50 [100]	0.01 [0.7]	0.75 [50]	0.74 [49.3]	0.68
MCNT-TiO₂ (10:1)	87	188	1.92 [100]	0.01 [0.5]	1.11 [57.9]	0.80 [41.6]	0.45
MCNT-TiO₂ (5:1)	71	177	1.44 [100]	0.01 [0.7]	0.76 [52.9]	0.67 [46.4]	0.44
MCNT-TiO₂ (1:1)	51	156	1.26 [100]	0.01 [0.8]	0.66 [52.1]	0.59 [47.1]	0.41
MCNT-TiO₂ (1:5)	32	151	1.20 [100]	0.01 [0.8]	0.65 [54.4]	0.54 [44.8]	0.34
MCNT-TiO₂ (1:10)	28	144	1.18 [100]	0.01 [0.8]	0.61 [52]	0.56 [47.2]	0.33

SA: surface area; PV_{total}: total pore volume; PV_{micro}: volume of micropores (PV < 2 nm); PV_{meso}: volume of mesopores (2 < PV 50 nm); and PV_{macro}: volume of macropores (PV > 50 nm).
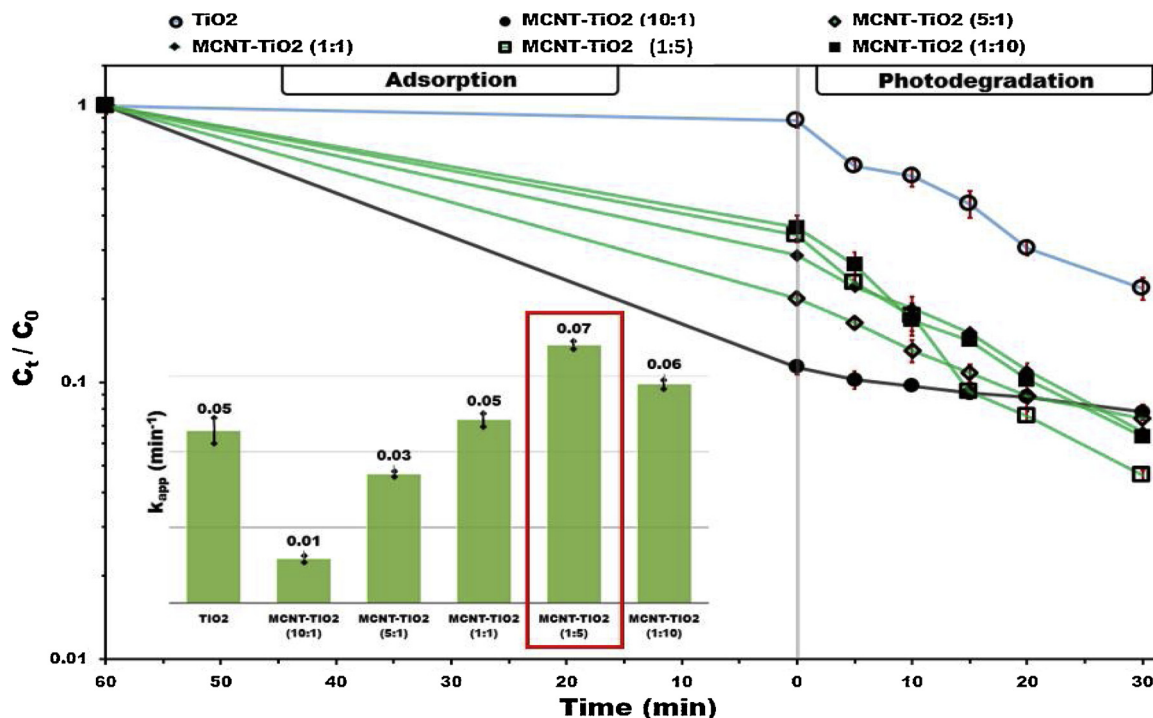

Fig. 2. Adsorption and photodegradation of carbamazepine for each photocatalyst (Co = 150 μg L^{-1}, solar irradiation time = 30 min, catalyst dose = 0.1 g L^{-1}, pH = 7 ± 0.2, temperature = 26 ± 3 °C). Inset graphs show the photodegradation rate. The values in the brackets following the composite name show the MCNT:TiO₂ mass ratio. Data and error bars indicate the average and standard deviation from duplicate experiments.

electrons into TiO₂ which increases the photocurrent, 2) the excitation electron from MCNT can combine with dissolved O₂ to form superoxide, and 3) MCNT provides suitable sites for the sorption of contaminants, acts as an electron sink, and renders visible light absorption due to Ti-O-C linkage (i.e., band gap reduction). However, increasing the TiO₂:MCNT mass ratio further (MCNT-TiO₂ (1:10)) reduced the degradation efficiency, mainly because of the aggregation of TiO₂ on the MCNTs, which limited the number of active sites for sorption and photocatalysis [45]. Moreover, an excessive amount of MCNTs (MCNT-TiO₂ (10:1) and MCNT-TiO₂ (5:1)) also decreased the photodegradation rate of carbamazepine by screening the light and preventing the photocatalytic reaction [46]. Therefore, MCNT-TiO₂ (1:5) was selected for the subsequent experiments as the optimum MCNT:TiO₂ mass ratio for achieving the maximum photocatalytic degradation of the target contaminants.

We evaluated the photodegradation rate at initial concentrations of carbamazepine and sulfamethoxazole of 150 and 500 μg L^{-1}. The photodegradation rate of carbamazepine decreased significantly at the higher initial concentrations for both TiO₂ and MCNT-TiO₂ (p < 0.01) (Fig. S9). This reduction may be related to the absorption of light by carbamazepine and the degradation intermediates, which may interfere

with the photocatalytic degradation reaction. However, the effect of the increased initial concentration was small for sulfamethoxazole. Hydroxylation processes (i.e., hydroxyl radical oxidation) have been reported as a main degradation mechanism of carbamazepine by TiO₂-based photocatalysis [47,48]. In contrast, degradation mechanism for sulfamethoxazole happened due to hydroxylation process and also direct degradation (i.e., direct photolysis) via the cleavage of the S–N bond [41]. At fixed catalysts concentration and irradiation times, the total hydroxyl radicals amounts are constant [49]. Therefore, the effect of increased initial concentration at fixed catalyst concentration on the degradation rate was more prone in case of carbamazepine than sulfamethoxazole; where direct photolysis also take part in the total degradation rate for the latter case.

3.3. Adsorption and photodegradation of pharmaceuticals in the presence of NOM

The presence of NOM is of particular concern because it competes for the adsorption sites and quenches advanced oxidation processes [50]. The photocatalytic degradation of carbamazepine (Fig. 3) and sulfamethoxazole (Fig. S10) using TiO₂ and MCNT-TiO₂ (1:5) was tested
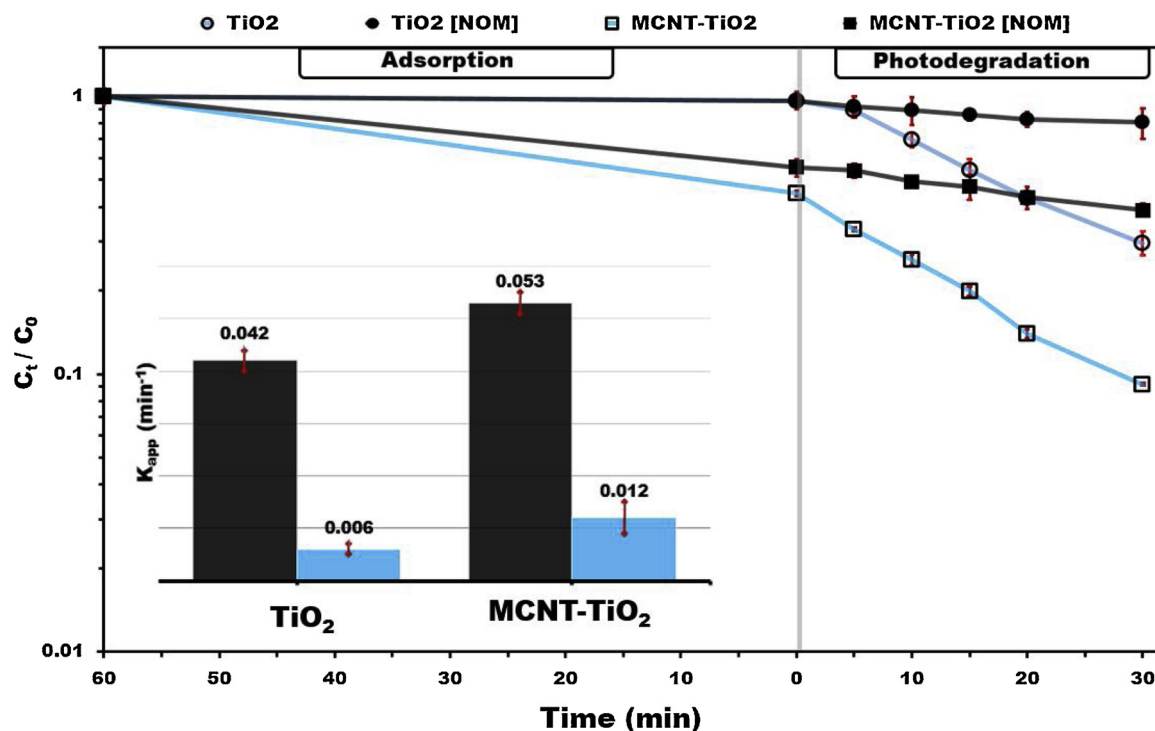
Fig. 3. Adsorption and photodegradation of carbamazepine at an initial concentration of 500 µg L^{-1} in the presence of NOM (DOC = 5 mg DOC L^{-1}, solar irradiation time = 30 min, catalyst dose = 0.1 g L^{-1}, pH = 7 ± 0.2). Inset graphs show the photodegradation rate. Data and error bars indicate the average and standard deviation from duplicate experiments.

in the presence of NOM, which significantly decreased the adsorption of carbamazepine and sulfamethoxazole onto TiO$_2$ and MCNT-TiO$_2$ (1:5) (p < 0.05). The competitive adsorption of NOM reduced the interaction between the pharmaceuticals and the catalysts [16]. These observations also confirmed the advantage of using MCNT-TiO$_2$, because, despite the competition, the high surface area of the composites provided enough active sites for the adsorption of carbamazepine and sulfamethoxazole on MCNT-TiO$_2$ in contrast to TiO$_2$. The heterogeneous nature of NOM affects the molecular sieving behavior of TiO$_2$ and CNTs. In the presence of NOM, TiO$_2$ preferentially adsorbs small to medium molecular weight species (> 0.1 kDa) [15], whereas CNTs adsorb species with molecular weights of 1–3 kDa [39].

The presence of NOM significantly reduced the photodegradation rate of TiO$_2$ for carbamazepine and sulfamethoxazole from 4.2×10^{-2} and 4.7×10^{-2} min^{-1}, respectively, in the absence of NOM, to 6×10^{-3} and 5×10^{-3} min^{-1} (p < 0.01). For MCNT-TiO$_2$ (1:5), the photodegradation rates of carbamazepine and sulfamethoxazole were also decreased significantly from 5.3×10^{-2} and 4.9×10^{-2} min^{-1}, respectively, in the absence of NOM, to 1.2×10^{-2} and 7×10^{-3} min^{-1}, respectively (p < 0.01). The significant decrease in photodegradation rates of carbamazepine and sulfamethoxazole were due to competitive adsorption [51], scavenger effect of NOM toward ˙OH radicals [17] and superoxide [52], as well as absorbing light via the inner filter effect [53,54]. NOM absorbs in both the UV and visible light spectrum, diminishing the illumination intensity that available for the production of reactive oxygen species (ROS). Further, the non-selective nature of ˙OH radicals and superoxide lead to the ROS loss due to reaction with either the targeted pharmaceuticals or the non-targeted compounds (i.e., background NOM). Besides those reasons, the adsorbed NOM (i.e., electron-rich compounds) were also capable of scavenging the holes (h^+) in the catalysts valence band and reduced the interaction of the pharmaceuticals close to the catalysts active site for the photodegradation processes [16]. The inhibitory effect of NOM depends strongly on the properties of the target compounds, NOM quality and quantity, and the catalysts. In our study, despite the lower

photodegradation rate in the presence of NOM, the reductions in the removal efficiency and the photodegradation rate of MCNT-TiO$_2$ (1:5) were less than those of bare TiO$_2$ under the operational conditions. These findings highlight the effect of NOM on the photocatalytic degradation using MCNT-TiO$_2$, although future studies will be necessary to understand fully the effects of NOM types and concentrations on the removal efficacy of photocatalytic degradation.

The comparison of photocatalytic performance of fabricated MCNT-TiO$_2$ with peer CNT-TiO$_2$ composites is summarized in Table S1. Previous studies set out that the total removal of pharmaceuticals was ranging from 50 to 99% for various CNT-TiO$_2$ composites. However, the removal of carbamazepine and sulfamethoxazole from this study were > 60% and > 40%, respectively. The photocatalytic activity of CNT-TiO2 composites mainly related with the photocatalysts morphologies, pharmaceuticals physicochemical properties, initial concentrations of pharmaceuticals, source of the lights or intensities, and the effect of water chemistries (e.g., pH, background co-existing organic or inorganic species) [14]. It was noted that most of the previous studies evaluate the photocatalytic activity of CNT-TiO$_2$ under UV irradiation (λ_{max} = 254–366) and in ultrapure water matrices. Therefore, this different might be largely because the difference in the source of the light and the water matrices. Compared with the others, the fabricated MCNT-TiO$_2$ in this study exhibits a promising photocatalytic performance under solar irradiation and in the presence of co-existing background NOM.

3.4. Recyclability of the MCNT-TiO$_2$ composite

The recyclability of MCNT-TiO$_2$ (1:5) was investigated by repeating the carbamazepine and sulfamethoxazole photodegradation experiments in the absence of NOM for five cycles of treatment and cleaning (Fig. 4). Photoreactivation by solar and UVC regeneration were used in this study, where UVC regeneration gave the best performance, probably due to the higher energy for the production of radicals. The carbamazepine and sulfamethoxazole removal tended to decrease from the
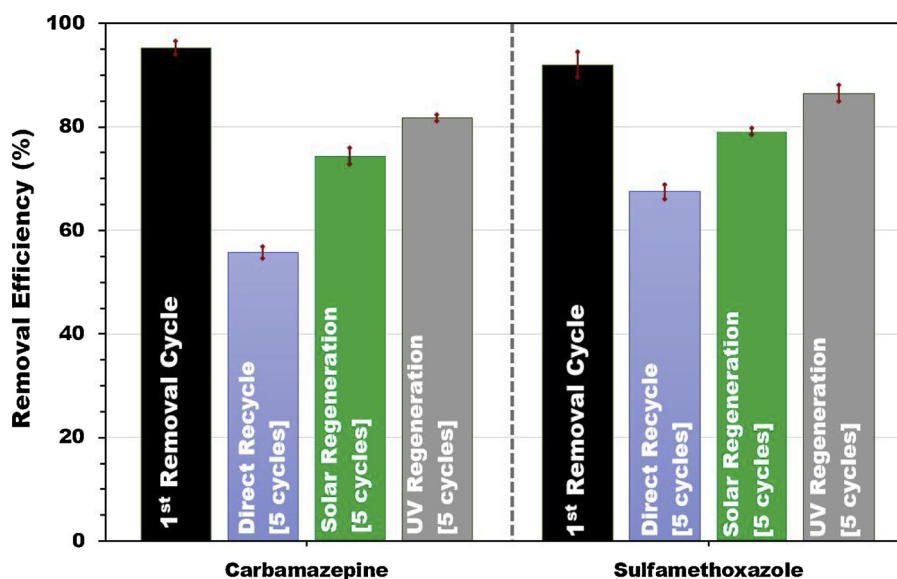
Fig. 4. Results for the regeneration scenarios for MCNT-TiO$_2$ $_{(1:5)}$ for carbamazepine and sulfamethoxazole photodegradation at an initial concentration of 150 μg L^{-1} (catalyst dose = 0.1 g/L, pH = 7 ± 0.2, temperature = 26 ± 3 °C). Data and error bars indicate the average and standard deviation from duplicate experiments.

first to the fifth cycle for all of the conditions. Direct recycling of MCNT-TiO$_2$ $_{(1:5)}$ statistically showed the highest decrease in the percentage removal of carbamazepine (~40% decrease after five cycles), followed by solar regeneration (~20% decrease after five cycles), and UVC regeneration (~15% decrease after five cycles) ($p < 0.001$). A similar trend was observed for sulfamethoxazole, where UVC regeneration statistically gave the lowest decrease in the removal efficiency after five cycles ($p < 0.001$). Sulfamethoxazole also showed a lower decrease in removal efficiencies after five cycles than carbamazepine for direct recycling, solar regeneration, and UVC regeneration. These results agree with a previous study [55], in which pharmaceuticals with F- and S-containing groups (e.g., sulfamethoxazole) were more rapidly photodegraded and regenerated than molecules without these groups (carbamazepine) in TiO$_2$ photocatalysis. The decrease in percentage removal of carbamazepine and sulfamethoxazole may be due to the accumulation of carbamazepine and sulfamethoxazole or their photodegradation byproducts on MCNT-TiO$_2$ $_{(1:5)}$ [56].

3.5. Electrical energy determination

The photochemical process of contaminant degradation is energy intensive and the electrical energy per order (E_{EO}) represents a major fraction of the total operating cost [57]. This approach allows a simple comparison, and provides data required for scale-up and economic analysis. However, comprehensive information about the use of E_{EO} values in modified TiO$_2$-based photocatalysis applications is still limited [29]. The E_{EO} values calculated for carbamazepine and sulfamethoxazole removal in ultrapure water and in the presence of NOM are shown in Fig. 5.

In general, the photocatalysis techniques gave lower electrical consumptions than photolysis for the degradation of the pharmaceuticals, mainly due to the production of radicals, which increased the degradation rate. The electrical energy consumption for the photocatalytic process in the presence of NOM was higher than that without NOM. The electrical energy consumption depended on the water quality (e.g., presence of NOM) and the pharmaceutical properties (stable or prone to direct photodegradation) because photolysis and photocatalysis are compound-specific processes [58]. Moreover, E_{EO} values of 2076–19,954 kW h m^{-3} order^{-1} were necessary to transform carbamazepine and sulfamethoxazole in ultrapure water and in the presence of NOM using pristine TiO$_2$, whereas lower E_{EO} values of

1820–15,054 kW h m^{-3} order^{-1} were needed for MCNT-TiO$_2$ due to the synergetic effect between MCNTs and TiO$_2$ in the composite system. It should be noted that these calculated E_{EO} values were used for comparison purposes and they may differ in real water samples where inorganic species are present.

4. Conclusions

We used a solar-light-driven MCNT-TiO$_2$ composite for the photocatalytic degradation of carbamazepine and sulfamethoxazole. An optimum mass ratio of MCNT to TiO$_2$ was needed to achieve maximum photodegradation of pharmaceuticals. The recyclability of MCNT-TiO$_2$ was assessed through five consecutive cycles of treatment and cleaning. The removal efficiency decreased as the number of consecutive cycles increased due to MCNT-TiO$_2$ fouling. To recover the photocatalytic efficiency, solar and UVC irradiation were used for regeneration. UVC irradiation showed better performance than solar irradiation. Finally, MCNT-TiO$_2$ was tested under more realistic conditions in the presence of NOM, and MCNT-TiO$_2$ still degraded carbamazepine and sulfamethoxazole. Compared with pristine TiO$_2$, the photocatalytic activity of MCNT-TiO$_2$ was higher and the electrical energy consumption was lower. Future studies should test MCNT-TiO$_2$ for the removal of other organic micropollutants (e.g., pharmaceuticals, personal care products, pesticides, dyes, etc.) in real waters and/or wastewaters and for the identification of the pathway and the toxicity of the degradation byproducts.

Appendix A. Supplementary data

Supplementary material related to this article can be found, in the online version, at doi:https://doi.org/10.1016/j.jwpe.2019.100836.
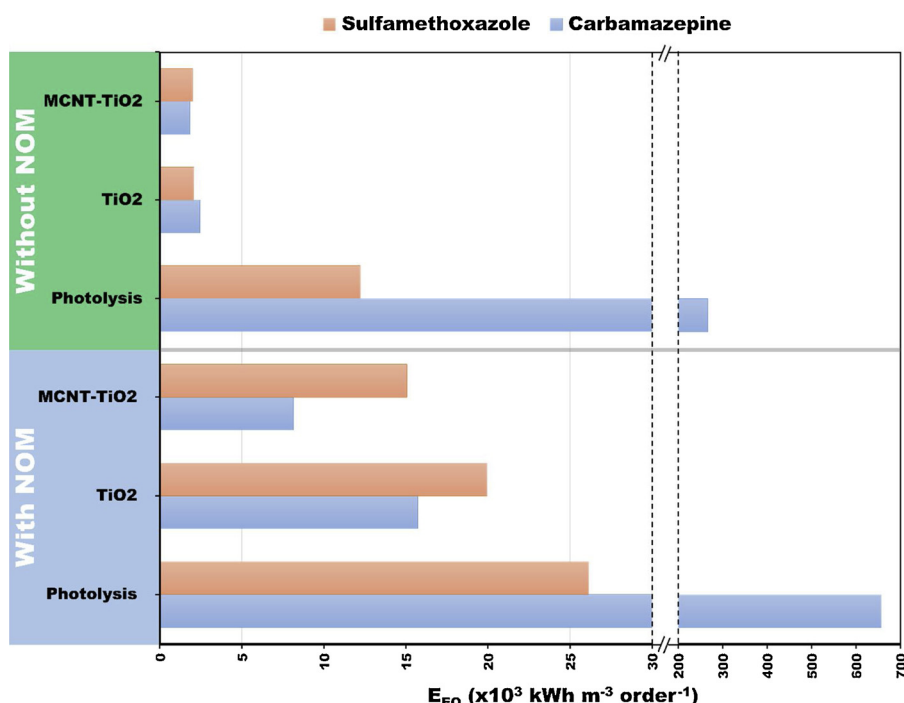
■ **Sulfamethoxazole** ■ **Carbamazepine**

Fig. 5. Electrical energy per order of transformation of carbamazepine (CBZ) and sulfamethoxazole (SMZ) at an initial concentration of $500\,\mu g\,L^{-1}$ for photolysis and photocatalysis in ultrapure water and in the presence of NOM. (DOC = $5\,mg\,DOC\,L^{-1}$, solar irradiation time = 30 min, catalysts dose = $0.1\,g\,L^{-1}$, pH = $7.0\,\pm\,0.2$, temperature = $26\,\pm\,3\,°C$).

References

[1] J.Q. Jiang, Z. Zhou, V.K. Sharma, Occurrence, transportation, monitoring and treatment of emerging micro-pollutants in waste water – a review from global views, Microchem. J. 110 (2013) 292–300, https://doi.org/10.1016/j.microc.2013.04.014.

[2] Y. Lester, H. Mamane, I. Zucker, D. Avisar, Treating wastewater from a pharmaceutical formulation facility by biological process and ozone, Water Res. 47 (2013) 4349–4356, https://doi.org/10.1016/j.watres.2013.04.059.

[3] M. Galus, J. Jeyaranjaan, E. Smith, H. Li, C. Metcalfe, J.Y. Wilson, Chronic effects of exposure to a pharmaceutical mixture and municipal wastewater in zebrafish, Aquat. Toxicol. 132–133 (2013) 212–222, https://doi.org/10.1016/j.aquatox.2012.12.016.

[4] J. Schwaiger, H. Ferling, U. Mallow, H. Wintermayr, R.D. Negele, Toxic effects of the non-steroidal anti-inflammatory drug diclofenac. Part I: histopathological alterations and bioaccumulation in rainbow trout, Aquat. Toxicol. 68 (2004) 141–150, https://doi.org/10.1016/j.aquatox.2004.03.014.

[5] A. Lagesson, J. Fahlman, T. Brodin, J. Fick, M. Jonsson, P. Byström, J. Klaminder, Bioaccumulation of five pharmaceuticals at multiple trophic levels in an aquatic food web – insights from a field experiment, Sci. Total Environ. 568 (2016) 208–215, https://doi.org/10.1016/j.scitotenv.2016.05.206.

[6] Y. Yang, Y.S. Ok, K.-H. Kim, E.E. Kwon, Y.F. Tsang, Occurrences and removal of pharmaceuticals and personal care products (PPCPs) in drinking water and water/sewage treatment plants: a review, Sci. Total Environ. 596–597 (2017) 303–320, https://doi.org/10.1016/j.scitotenv.2017.04.102.

[7] Y. Luo, W. Guo, H.H. Ngo, L.D. Nghiem, F.I. Hai, J. Zhang, S. Liang, X.C. Wang, A review on the occurrence of micropollutants in the aquatic environment and their fate and removal during wastewater treatment, Sci. Total Environ. 473–474 (2014) 619–641, https://doi.org/10.1016/j.scitotenv.2013.12.065.

[8] N. Jallouli, L.M. Pastrana-Martínez, A.R. Ribeiro, N.F.F. Moreira, J.L. Faria, O. Hentati, A.M.T. Silva, M. Ksibi, Heterogeneous photocatalytic degradation of ibuprofen in ultrapure water, municipal and pharmaceutical industry wastewaters using a TiO2/UV-LED system, Chem. Eng. J. 334 (2018) 976–984, https://doi.org/10.1016/j.cej.2017.10.045.

[9] D. Kanakaraju, C.A. Motti, B.D. Glass, M. Oelgemöller, TiO2 photocatalysis of naproxen: effect of the water matrix, anions and diclofenac on degradation rates, Chemosphere 139 (2015) 579–588, https://doi.org/10.1016/j.chemosphere.2015.07.070.

[10] Y. Chen, K. Liu, Preparation and characterization of nitrogen-doped TiO2/diatomite integrated photocatalytic pellet for the adsorption-degradation of tetracycline hydrochloride using visible light, Chem. Eng. J. 302 (2016) 682–696, https://doi.org/10.1016/j.cej.2016.05.108.

[11] M.N. Chong, B. Jin, C.W.K. Chow, C. Saint, Recent developments in photocatalytic water treatment technology: a review, Water Res. 44 (2010) 2997–3027, https://doi.org/10.1016/j.watres.2010.02.039.

[12] A.T. Kuvarega, B.B. Mamba, TiO2-based photocatalysis: toward visible light-responsive photocatalysts through doping and fabrication of carbon-based nanocomposites, Crit. Rev. Solid State Mater. Sci. 0 (2016) 1–52, https://doi.org/10.1080/10408436.2016.1211507.

[13] W. Wang, P. Serp, P. Kalck, J.L. Faria, Visible light photodegradation of phenol on MWNT-TiO2 composite catalysts prepared by a modified sol-gel method, J. Mol. Catal. A Chem. 235 (2005) 194–199, https://doi.org/10.1016/j.molcata.2005.02.027.

[14] D. Awfa, M. Ateia, M. Fujii, M.S. Johnson, C. Yoshimura, Photodegradation of pharmaceuticals and personal care products in water treatment using carbonaceous-TiO2 composites: a critical review of recent literature, Water Res. 142 (2018) 1–77, https://doi.org/10.1016/j.watres.2018.05.036.

[15] M. Drosos, M. Ren, F.H. Frimmel, The effect of NOM to TiO2: interactions and photocatalytic behavior, Appl. Catal. B Environ. 165 (2015) 328–334, https://doi.org/10.1016/j.apcatb.2014.10.017.

[16] M. Ren, M. Drosos, F.H. Frimmel, Inhibitory effect of NOM in photocatalysis process: explanation and resolution, Chem. Eng. J. 334 (2018) 968–975, https://doi.org/10.1016/j.cej.2017.10.099.

[17] J. Brame, M. Long, Q. Li, P. Alvarez, Inhibitory effect of natural organic matter or other background constituents on photocatalytic advanced oxidation processes: mechanistic model development and validation, Water Res. 84 (2015) 362–371, https://doi.org/10.1016/j.watres.2015.07.044.

[18] M. Ateia, C. Koch, S. Jelavić, A. Hirt, J. Quinson, C. Yoshimura, M. Johnson, Green and facile approach for enhancing the inherent magnetic properties of carbon nanotubes for water treatment applications, PLoS One 12 (2017) e0180636, , https://doi.org/10.1371/journal.pone.0180636.

[19] M. Ateia, M. Ceccato, A. Budi, E. Ataman, C. Yoshimura, M.S. Johnson, Ozone-assisted regeneration of magnetic carbon nanotubes for removing organic water pollutants, Chem. Eng. J. 335 (2018) 384–391, https://doi.org/10.1016/j.cej.2017.10.166.

[20] S.M. Miranda, G.E. Romanos, V. Likodimos, R.R.N. Marques, E.P. Favvas, F.K. Katsaros, K.L. Stefanopoulos, V.J.P. Vilar, J.L. Faria, P. Falaras, A.M.T. Silva, Pore structure, interface properties and photocatalytic efficiency of hydration/dehydration derived TiO2/CNT composites, Appl. Catal. B Environ. 147 (2014) 65–81, https://doi.org/10.1016/j.apcatb.2013.08.013.

[21] Y. Yao, G. Li, S. Ciston, R.M. Lueptow, K.A. Gray, Photoreactive TiO2/carbon nanotube composites: synthesis and reactivity, Environ. Sci. Technol. 42 (2008) 4952–4957, https://doi.org/10.1021/es800191n.

[22] G. Daneshvar Tarigh, F. Shemirani, N.S. Maz'hari, Fabrication of a reusable magnetic multi-walled carbon nanotube–TiO2 nanocomposite by electrostatic adsorption: enhanced photodegradation of malachite green, RSC Adv. 5 (2015) 35070–35079, https://doi.org/10.1039/C4RA15593A.

[23] C.A. Orge, J.L. Faria, M.F.R. Pereira, Photocatalytic ozonation of aniline with TiO2-carbon composite materials, J. Environ. Manage. (2016) 1–8, https://doi.org/10.1016/j.jenvman.2016.07.091.

[24] P.S. Yap, T.T. Lim, Solar regeneration of powdered activated carbon impregnated with visible-light responsive photocatalyst: factors affecting performances and predictive model, Water Res. 46 (2012) 3054–3064, https://doi.org/10.1016/j.watres.2012.03.008.

[25] O. Cardoso, J.M. Porcher, W. Sanchez, Factory-discharged pharmaceuticals could be a relevant source of aquatic environment contamination: review of evidence and need for knowledge, Chemosphere. 115 (2014) 20–30, https://doi.org/10.1016/j.chemosphere.2014.02.004.

[26] Y.P. Lee, M. Fujii, T. Kikuchi, K. Terao, C. Yoshimura, Variation of iron redox kinetics and its relation with molecular composition of standard humic substances at circumneutral pH, PLoS One 12 (2017) 1–21, https://doi.org/10.1371/journal.

pone.0176484.

[27] J. Raeke, O.J. Lechtenfeld, B. Seiwert, T. Meier, C. Riemenschneider, T. Reemtsma, Photochemically induced bound residue formation of carbamazepine with dissolved organic matter, Environ. Sci. Technol. 51 (2017) 5523–5530, https://doi.org/10.1021/acs.est.7b00823.

[28] S. Carbonaro, M.N. Sugihara, T.J. Strathmann, Continuous-flow photocatalytic treatment of pharmaceutical micropollutants: activity, inhibition, and deactivation of TiO_2 photocatalysts in wastewater effluent, Appl. Catal. B Environ. 129 (2013) 1–12, https://doi.org/10.1016/j.apcatb.2012.09.014.

[29] D.B. Miklos, C. Remy, M. Jekel, K.G. Linden, J.E. Drewes, U. Hübner, Evaluation of advanced oxidation processes for water and wastewater treatment – a critical review, Water Res. 139 (2018) 118–131, https://doi.org/10.1016/j.watres.2018.03.042.

[30] J. Vejpravova, B. Pacakova, M. Kalbac, Magnetic impurities in single-walled carbon nanotubes and graphene: a review, Analyst 141 (2016) 2639–2656, https://doi.org/10.1039/C6AN00248J.

[31] P. Zhang, Z. Mo, L. Han, Y. Wang, G. Zhao, C. Zhang, Z. Li, Magnetic recyclable TiO_2/multi-walled carbon nanotube nanocomposite: synthesis, characterization and enhanced photocatalytic activity, J. Mol. Catal. A Chem. 402 (2015) 17–22, https://doi.org/10.1016/j.molcata.2015.03.005.

[32] Y. Luo, Z. Lu, Y. Jiang, D. Wang, L. Yang, P. Huo, Z. Da, X. Bai, X. Xie, P. Yang, Selective photodegradation of 1-methylimidazole-2-thiol by the magnetic and dual conductive imprinted photocatalysts based on TiO_2/Fe_3O_4/MWCNTs, Chem. Eng. J. 240 (2014) 244–252, https://doi.org/10.1016/j.cej.2013.11.088.

[33] Q.H. Yang, P.X. Hou, H.M. Cheng, Adsorption and capillarity of nitrogen in inside channel of carbon nanotubes, Abstr. Pap. Am. Chem. Soc. 221 (2001) U581–U581.

[34] J. Yu, H. Yu, B. Cheng, M. Zhou, X. Zhao, Enhanced photocatalytic activity of TiO_2 powder (P25) by hydrothermal treatment, J. Mol. Catal. A Chem. 253 (2006) 112–118, https://doi.org/10.1016/j.molcata.2006.03.021.

[35] C. He, S. Qiu, X. Wang, J. Liu, L. Luan, W. Liu, M. Itoh, K.I. MacHida, Facile synthesis of hollow porous cobalt spheres and their enhanced electromagnetic properties, J. Mater. Chem. 22 (2012) 22160–22166, https://doi.org/10.1039/c2jm33068g.

[36] Y. Ye, Y. Feng, H. Bruning, D. Yntema, H.H.M. Rijnaarts, Photocatalytic degradation of metoprolol by TiO_2 nanotube arrays and UV-LED: effects of catalyst properties, operational parameters, commonly present water constituents, and photo-induced reactive species, Appl. Catal. B Environ. 220 (2018) 171–181, https://doi.org/10.1016/j.apcatb.2017.08.040.

[37] S. Wang, S. Zhou, Photodegradation of methyl orange by photocatalyst of CNTs/P-TiO_2 under UV and visible-light irradiation, J. Hazard. Mater. 185 (2011) 77–85, https://doi.org/10.1016/j.jhazmat.2010.08.125.

[38] K. Yang, B. Xing, Adsorption of fulvic acid by carbon nanotubes from water, Environ. Pollut. 157 (2009) 1095–1100, https://doi.org/10.1016/j.envpol.2008.11.007.

[39] M. Ateia, O.G. Apul, Y. Shimizu, A. Muflihah, C. Yoshimura, T. Karanfil, Elucidating adsorptive fractions of natural organic matter on carbon nanotubes, Environ. Sci. Technol. 51 (2017) 7101–7110, https://doi.org/10.1021/acs.est.7b01279.

[40] S.K. Maeng, K. Cho, B. Jeong, J. Lee, Y. Lee, C. Lee, K.J. Choi, S.W. Hong, Substrate-immobilized electrospun TiO_2 nanofibers for photocatalytic degradation of pharmaceuticals: the effects of pH and dissolved organic matter characteristics, Water Res. 86 (2015) 25–34, https://doi.org/10.1016/j.watres.2015.05.032.

[41] H. Zhang, Z. Wang, R. Li, J. Guo, Y. Li, J. Zhu, X. Xie, TiO_2 supported on reed straw biochar as an adsorptive and photocatalytic composite for the efficient degradation of sulfamethoxazole in aqueous matrices, Chemosphere 185 (2017) 351–360, https://doi.org/10.1016/j.chemosphere.2017.07.025.

[42] Y. Wang, F.A. Roddick, L. Fan, Direct and indirect photolysis of seven micro-pollutants in secondary effluent from a wastewater lagoon, Chemosphere 185 (2017) 297–308, https://doi.org/10.1016/j.chemosphere.2017.06.122.

[43] A.L. Boreen, W.A. Arnold, K. McNeill, Photochemical fate of sulfa drugs in then aquatic environment: sulfa drugs containing five-membered heterocyclic groups, Environ. Sci. Technol. 38 (2004) 3933–3940, https://doi.org/10.1021/es0353053.

[44] J. Herrmann, Heterogeneous photocatalysis: fundamentals and applications to the removal of various types of aqueous pollutants, Catal. Today 53 (1999) 115–129, https://doi.org/10.1016/S0920-5861(99)00107-8.

[45] C. Song, P. Chen, C. Wang, L. Zhu, Photodegradation of perfluorooctanoic acid by synthesized TiO_2-MWCNT composites under 365 nm UV irradiation, Chemosphere 86 (2012) 853–859, https://doi.org/10.1016/j.chemosphere.2011.11.034.

[46] F. Wang, K. Zhang, Reduced graphene oxide–TiO_2 nanocomposite with high photocatalystic activity for the degradation of rhodamine B, J. Mol. Catal. A Chem. 345 (2011) 101–107, https://doi.org/10.1016/j.molcata.2011.05.026.

[47] M. Nawaz, W. Miran, J. Jang, D.S. Lee, One-step hydrothermal synthesis of porous 3D reduced graphene oxide/TiO_2 aerogel for carbamazepine photodegradation in aqueous solution, Appl. Catal. B Environ. 203 (2017) 85–95, https://doi.org/10.1016/j.apcatb.2016.10.007.

[48] M.M. Dong, R. Trenholm, F.L. Rosario-Ortiz, Photochemical degradation of atenolol, carbamazepine, meprobamate, phenytoin and primidone in wastewater effluents, J. Hazard. Mater. 282 (2015) 216–223, https://doi.org/10.1016/j.jhazmat.2014.04.028.

[49] J. Carbajo, A. Tolosana-Moranchel, J.A. Casas, M. Faraldos, A. Bahamonde, Analysis of photoefficiency in TiO_2 aqueous suspensions: effect of titania hydrodynamic particle size and catalyst loading on their optical properties, Appl. Catal. B Environ. 221 (2018) 1–8, https://doi.org/10.1016/j.apcatb.2017.08.032.

[50] S.P. Sahu, M. Qanbarzadeh, M. Ateia, H. Torkzadeh, A.S. Maroli, E.L. Cates, Rapid degradation and mineralization of perfluorooctanoic acid by a new petitjeanite $Bi_3O(OH)(PO_4)_2$ microparticle ultraviolet photocatalyst, Environ. Sci. Technol. Lett. (2018), https://doi.org/10.1021/acs.estlett.8b00395 acs.estlett.8b00395.

[51] S. Li, J. Hu, Transformation products formation of ciprofloxacin in UVA/LED and UVA/LED/TiO_2 systems: impact of natural organic matter characteristics, Water Res. 132 (2018) 320–330, https://doi.org/10.1016/j.watres.2017.12.065.

[52] M. Fujii, E. Otani, Photochemical generation and decay kinetics of superoxide and hydrogen peroxide in the presence of standard humic and fulvic acids, Water Res. 123 (2017) 642–654, https://doi.org/10.1016/j.watres.2017.07.015.

[53] L.C. Bodhipaksha, C.M. Sharpless, Y.-P. Chin, A.A. MacKay, Role of effluent organic matter in the photochemical degradation of compounds of wastewater origin, Water Res. 110 (2017) 170–179, https://doi.org/10.1016/j.watres.2016.12.016.

[54] S. Yan, B. Yao, L. Lian, X. Lu, S.A. Snyder, R. Li, W. Song, Development of fluorescence surrogates to predict the photochemical transformation of pharmaceuticals in wastewater effluents, Environ. Sci. Technol. (2017), https://doi.org/10.1021/acs.est.6b05251 acs.est.6b05251.

[55] N. Miranda-García, S. Suárez, M.I. Maldonado, S. Malato, B. Sánchez, Regeneration approaches for TiO_2 immobilized photocatalyst used in the elimination of emerging contaminants in water, Catal. Today 230 (2014) 27–34, https://doi.org/10.1016/j.cattod.2013.12.048.

[56] R. De Sun, A. Nakajima, T. Watanabe, K. Hashimoto, Decomposition of gas-phase octamethyltrisiloxane on TiO_2 thin film photocatalysts – catalytic activity, deactivation, and regeneration, J. Photochem. Photobiol. A: Chem. 154 (2003) 203–209, https://doi.org/10.1016/S1010-6030(02)00322-2.

[57] M.A. Vishnuganth, N. Remya, M. Kumar, N. Selvaraju, Photocatalytic degradation of carbofuran by TiO_2-coated activated carbon: model for kinetic, electrical energy per order and economic analysis, J. Environ. Manage. 181 (2016) 201–207, https://doi.org/10.1016/j.jenvman.2016.06.016.

[58] L. Paredes, S. Murgolo, H. Dzinun, M.H. Dzarfan Othman, A.F. Ismail, M. Carballa, G. Mascolo, Application of immobilized TiO_2 on PVDF dual layer hollow fibre membrane to improve the photocatalytic removal of pharmaceuticals in different water matrices, Appl. Catal. B Environ. 240 (2019) 9–18, https://doi.org/10.1016/j.apcatb.2018.08.067.